XI International Conference on Computational Plasticity. Fundamentals and Applications
COMPLAS XI
E. Oñate, D.R.J. Owen, D. Peric and B. Suárez (Eds)

A COMPUTATIONAL PROCEDURE FOR THE CYCLIC STEADY STATE ELASTOPLASTIC ANALYSIS OF STRUCTURES - COMPLAS XI

KONSTANTINOS V. SPILIOPOULOS[*], KONSTANTINOS D. PANAGIOTOU[†]

[*] Institute of Structural Analysis and Antiseismic Research
National Technical University of Athens (NTUA)
Zografou Campus, 157 80 Athens, Greece
e-mail: kvspilio@central.ntua.gr; web page: http://users.ntua.gr/kvspilio/

[†] Institute of Structural Analysis and Antiseismic Research
National Technical University of Athens (NTUA)
Zografou Campus, 157 80 Athens, Greece
e-mail: dinoscivil@hotmail.com

Key words: Computational Plasticity, Cyclic Plasticity, Direct Method, Cyclic Loading, Elastic Adaptation, Alternating Plasticity, Incremental Collapse.

Abstract. A new computational procedure for the steady state elastoplastic analysis of structures under cyclic loading is presented. The procedure is based on the decomposition of the unknown steady state residual stress distribution into Fourier series. The coefficients of the series are evaluated in an iterative way by satisfying equilibrium and compatibility at some preselected time points inside the cycle. The procedure in the present work is applied to a simple 1-D three bar structure and to a 2-D plate. Various load cases are examined which may lead to elastic adaptation, alternating plasticity or incremental collapse.

1 INTRODUCTION

Structures such as nuclear reactors, aircraft gas turbine propulsion engines, etc. operate in high levels of loads and temperature. High levels of loading exist also in civil engineering structures like heavy traffic on bridges and pavements, earthquake loading etc.

The complete response of a structure, which is subjected to a given thermo-mechanical loading and exhibits inelastic time independent plastic strains, is quite complex. The reason of the complexity is the need to perform calculations over the lifetime history of the structure. The computation of the whole loading history, however, leads to lengthy and expensive incremental calculations, especially for structures with large number of degrees of freedom. Therefore, it is very useful to develop computational approaches for straightforward calculations of the possible stabilized state under repeated thermo-mechanical loading.

Direct cyclic methods offer this alternative. The ingredient of these methods is the existence of a steady state at the end of the loading procedure for structures made of ductile material [1].

The advantage that direct methods offer with respect to time-stepping ones has been exploited by many researchers. Most of these methods aim at the evaluation of the limit or the shakedown loading of a structure. This is normally done using the framework of linear or nonlinear mathematical programming and most of these approaches are reduced to efficiently solve this problem with the means of algorithms like the simplex method or more recently by the interior point methods([2]-[4]).

A different direct method of an incremental-iterative type has been presented in [5]. A more "physical" approach which is based on spatially varying of the elastic modulus is the Linear Matching Method. This method has been extended up to the ratchet limits ([6]-[8]).

A direct method has been proposed by Spiliopoulos [9] in the context of the cyclic loading analysis of creeping structures. The irreversibility of the nonlinear material dictates the existence of residual stresses together with the elastic stresses. It is the distribution of the residual stresses that is sought at the cyclic stress state. The method is based first on decomposing the unknown residual stress in Fourier series and then trying to find the coefficients of this series in an iterative way by satisfying equilibrium and compatibility at some preselected time points inside the cycle.

In the present work a computational procedure is proposed, that has the same foundations and may be applied to structures made of elastic perfectly plastic material. The whole procedure is formulated within the framework of the finite element method and examples of application to 1- and 2- dimensional structures are presented.

2 RESIDUAL STRESS DECOMPOSITION

The main ingredient of the method is the time decomposition of the unknown residual stress distribution $\boldsymbol{\rho}(t)$ into Fourier series. Since in the steady state this stress also becomes periodic, it may be decomposed in its Fourier series over the period of loading, as this can be done for any periodic function:

$$\boldsymbol{\rho}(t)=\frac{\boldsymbol{a}_0}{2}+\sum_{k=1}^{\infty}\left(\boldsymbol{a}_k\cos\frac{2k\pi t}{T}+\boldsymbol{b}_k\sin\frac{2k\pi t}{T}\right) \tag{1}$$

where the coefficients $\boldsymbol{a}_0$, $\boldsymbol{a}_k$ and $\boldsymbol{b}_k$, $k=1,2,...$ are the Fourier coefficients of the Fourier series. Vectors and matrices are denoted by bold letters.

Thus the problem is converted to a problem of evaluating the Fourier coefficients of the various terms of the series. Following, in short, the procedure developed in [9] we may get

$$\dot{\boldsymbol{\rho}}(t)=\frac{2\pi}{T}\sum_{k=1}^{\infty}\left\{(-k\boldsymbol{a}_k)\sin\frac{2k\pi t}{T}+k\boldsymbol{b}_k\cos\frac{2k\pi t}{T}\right\} \tag{2}$$

Making use of the orthogonality properties of the trigonometric functions we can get expressions that may be used to evaluate these coefficients in terms of the time derivative $\dot{\boldsymbol{\rho}}(t)$:

$$\boldsymbol{a}_k=-\frac{1}{k\pi}\int_0^T\dot{\boldsymbol{\rho}}(t)\sin\frac{2k\pi t}{T}dt \tag{3}$$

$$\boldsymbol{b}_k=\frac{1}{k\pi}\int_0^T\dot{\boldsymbol{\rho}}(t)\cos\frac{2k\pi t}{T}dt \tag{4}$$

On the other hand, if we integrate $\dot{\boldsymbol{\rho}}(t)$ over the period T, we get

$$\int_0^T \dot{\boldsymbol{\rho}}(t)\,dt = \boldsymbol{\rho}(T) - \boldsymbol{\rho}(0) = \left(\frac{\boldsymbol{\alpha}_0(T)}{2} + \sum_{k=1}^{\infty} \boldsymbol{\alpha}_k(T) \right) - \left(\frac{\boldsymbol{\alpha}_0(0)}{2} + \sum_{k=1}^{\infty} \boldsymbol{\alpha}_k(0) \right) \tag{5}$$

where use of the expression (1) was made at the beginning and at the end of the cycle period. Equation (5) may be used to evaluate the coefficient $\boldsymbol{a}_0$.

If one satisfies equilibrium and compatibility at some discrete preselected time points inside the cycle, the time derivatives of the residual stresses themselves may be expressed in terms of the Fourier coefficients we seek to find.

3 FINITE ELEMENT FORMULATION

In order to evaluate the time derivatives of the residual stresses we may discretize our structure with the aid of the finite element method.

Let us denote by $\dot{\boldsymbol{r}}$ the vector of the time rates of the time displacement of the nodal points of the discretized structure at some time t.

The total strain rates $\dot{\boldsymbol{\varepsilon}}$ at the Gauss integration points are given in term of $\dot{\boldsymbol{r}}$ by

$$\dot{\boldsymbol{\varepsilon}} = \boldsymbol{B}\dot{\boldsymbol{r}} \tag{6}$$

Decomposing $\dot{\boldsymbol{\varepsilon}}$ into two terms $\dot{\boldsymbol{e}}^{el}$ and $\dot{\boldsymbol{\varepsilon}}_r$

$$\dot{\boldsymbol{\varepsilon}} = \dot{\boldsymbol{e}}^{el} + \dot{\boldsymbol{\varepsilon}}_r = \dot{\boldsymbol{e}}^{el} + \dot{\boldsymbol{\varepsilon}}_r^{el} + \dot{\boldsymbol{\varepsilon}}_r^{pl} \tag{7}$$

In the above equation the residual strain rate term has been itself decomposed into elastic and plastic parts.

At the same time the stress also can be decomposed into two terms an elastic one and a residual stress part

$$\boldsymbol{\sigma}(t) = \boldsymbol{\sigma}^{el}(t) + \boldsymbol{\rho}(t) \tag{8}$$

The elastic strain rates are related to their corresponding stress rates by

$$\begin{aligned} \dot{\boldsymbol{e}}^{el} &= \boldsymbol{C}\dot{\boldsymbol{\sigma}}^{el} \\ \dot{\boldsymbol{\varepsilon}}_r^{el} &= \boldsymbol{C}\dot{\boldsymbol{\rho}} \end{aligned} \tag{9}$$

where $\boldsymbol{C}$ is the tensor of the elastic constants.

For the plastic component the associate flow rule gives

$$\dot{\boldsymbol{\varepsilon}}_r^{pl} = \lambda \frac{\partial \Phi}{\partial \boldsymbol{\sigma}} \tag{10}$$

where Φ is a strictly convex yield surface.

Combining the above equations (7) and (9) we may write

$$\dot{\boldsymbol{\rho}} = \boldsymbol{D}\left(\dot{\boldsymbol{\varepsilon}} - \dot{\boldsymbol{e}}^{el} - \dot{\boldsymbol{\varepsilon}}_r^{pl} \right) \tag{11}$$

where $\boldsymbol{D}$ is the elasticity matrix (inverse of $\boldsymbol{C}$).

Since the strain rates are compatible and the residual stress rates are self-equilibrated, from the principle of virtual work (P.V.W.) we may obtain

$$\int_V \dot{\boldsymbol{\varepsilon}}' \dot{\boldsymbol{\rho}} dV = 0 \tag{12}$$

where “ ′ ” denotes the transpose of a vector or a matrix.

After the substitution of (6) and (11), in (12) we get

$$\dot{\boldsymbol{r}}' \int_V \boldsymbol{B}' \boldsymbol{D}\left(\boldsymbol{B}\dot{\boldsymbol{r}} - \dot{\boldsymbol{e}}^{el} - \dot{\boldsymbol{\varepsilon}}_r^{pl}\right) dV = 0 \tag{13}$$

and since this equation must hold for any $\dot{\boldsymbol{r}}$

$$\left(\int_V \boldsymbol{B}' \boldsymbol{D}\boldsymbol{B} dV\right)\dot{\boldsymbol{r}} = \int_V \boldsymbol{B}' \dot{\boldsymbol{\sigma}}^{el} dV + \int_V \boldsymbol{B}' \boldsymbol{D}\dot{\boldsymbol{\varepsilon}}_r^{pl} dV \tag{14}$$

or

$$\boldsymbol{K}\dot{\boldsymbol{r}} = \dot{\boldsymbol{R}}^{ext} + \int_V \boldsymbol{B}' \boldsymbol{D}\dot{\boldsymbol{\varepsilon}}_r^{pl} dV \tag{15}$$

where $\boldsymbol{K}$ is the stiffness matrix of the structure and $\dot{\boldsymbol{R}}^{ext}$ is the nodal vector of the time rate of the given loading.

4 ITERATIVE PROCEDURE

The form of the expressions (3), (4) and (5) allow us to evaluate the Fourier series (1) in an iterative procedure. The proposed numerical procedure has the following steps during a current iteration μ :

1. Calculation of the total stresses $\boldsymbol{\sigma}^{(\mu)}(t) = \boldsymbol{\sigma}^{el}(t) + \boldsymbol{\rho}^{(\mu)}(t)$ at some preselected time points inside the cycle; $\boldsymbol{\sigma}^{el}(t)$ is the cyclic elastic stress and $\boldsymbol{\rho}^{(\mu)}(t)$ is a self equilibrating stress system due to plasticity.
2. Checking for every Gauss point if $\overline{\sigma}^{(\mu)}(t) > \sigma_Y$ and calculation of the amount $\Delta\boldsymbol{\sigma}^{(\mu)}(t) = \xi * \boldsymbol{\sigma}^{(\mu)}(t)$ where $\xi = \dfrac{\overline{\sigma}^{(\mu)}(t) - \sigma_Y}{\overline{\sigma}^{(\mu)}(t) - \overline{\rho}^{(\mu)}(t)}$. $\overline{\sigma}^{(\mu)}(t)$ and $\overline{\rho}^{(\mu)}(t)$ are the corresponding effective total and residual stresses, σ_Y is the yield stress. If $\overline{\sigma}^{(\mu)}(t) \le \sigma_Y$ we set $\xi = 0$ and continue to the next step.
3. Solving the expanded rate equilibrium equation $\boldsymbol{K}\dot{\boldsymbol{r}}^{(\mu)}(t) = \dot{\boldsymbol{R}}^{ext}(t) + \int_V \boldsymbol{B}^T \Delta\boldsymbol{\sigma}^{(\mu)}(t) dV$ where $\boldsymbol{B}$ is the compatibility matrix and $\dot{\boldsymbol{R}}^{ext}(t) \,\&\, \dot{\boldsymbol{r}}(t)$ are the corresponding vectors of the time rates of the external loads and displacements of the nodal points of the discretized structure at some time t. In this step we get the new vector $\dot{\boldsymbol{r}}(t)$
4. Calculation of $\dot{\boldsymbol{\rho}}^{(\mu)}(t) = \boldsymbol{D}\boldsymbol{B}\dot{\boldsymbol{r}}^{(\mu)}(t) - \dot{\boldsymbol{\sigma}}^{el}(t) - \Delta\boldsymbol{\sigma}^{(\mu)}(t)$.

5. Perform numerical time integration over all the time points and update the Fourier coefficients for the next iteration:

$$\begin{aligned} \boldsymbol{a}_k^{(\mu+1)} &= -\frac{1}{k\pi}\int_0^T \left\{ \left[\dot{\boldsymbol{\rho}}^{(\mu)}(t) \right] \left[sin\frac{2k\pi t}{T} \right] \right\} dt \\ \boldsymbol{b}_k^{(\mu+1)} &= \frac{1}{k\pi}\int_0^T \left\{ \left[\dot{\boldsymbol{\rho}}^{(\mu)}(t) \right] \left[cos\frac{2k\pi t}{T} \right] \right\} dt \\ \boldsymbol{a}_0^{(\mu+1)} &= -\sum_{k=1}^{\infty} \boldsymbol{a}_k^{(\mu+1)} + \frac{\boldsymbol{a}_0^{(\mu)}}{2} + \sum_{k=1}^{\infty} \boldsymbol{a}_k^{(\mu)} + \int_0^T \left[\dot{\boldsymbol{\rho}}^{(\mu)}(t) \right] dt \end{aligned} \tag{16}$$

6. Checking the convergence between two successive iterations using the Euclidian norm of the residual stress vector according to the following criterion:

$$\frac{\left\| \boldsymbol{\rho}^{(\mu+1)} \right\|_2 - \left\| \boldsymbol{\rho}^{(\mu)} \right\|_2}{\left\| \boldsymbol{\rho}^{(\mu+1)} \right\|_2} \le tol \tag{17}$$

where tol is a pre-specified tolerance. If convergence occurs we get the final stresses $\boldsymbol{\rho}^{(\mu)} = \boldsymbol{\rho}^{(\mu+1)} = \boldsymbol{\rho}^{(final)}$ and continue to the next step. Otherwise we go to the next iteration and return to the step 1.

7. In order to predict the cyclic behaviour of the structure we calculate the value $a = \left\| \int_0^T \Delta\boldsymbol{\sigma}^{(\mu)}(t)dt \right\|$.

If $a \neq 0$, the considered loading case leads the structure to *incremental collapse*.
If $a = 0$, we check if $\left\| \Delta\boldsymbol{\sigma}^{(\mu)}(t) \right\| = 0$ for every time point *t* inside the cycle. If this is the case we have *elastic adaptation*; otherwise we have *alternating plasticity*.

5 EXAMPLES

5.1 Three bar truss

A first example of application of the methodology presented above is the three bar structure which is shown in Fig. 1. The structure is subjected to cyclic loads $V(t)$, $H(t)$ which are applied at node 4. All the members of the truss have equal cross section A and are made of steel. The following geometrical, material data were used: $L = 300cm$, Young's modulus $E = .21 \times 10^5 kN/cm^2$ and yield stress $\sigma_y = 40kN/cm^2$. All the elements of the truss have an equal cross-sectional area of $A = 5cm^2$. Three cases of loading have been considered to test the procedure. Each of these cases leads to different cyclic behaviour. The results for the elements *1*, *3* are equal to the ones of element *2*, but with opposite sign.

a) The first cyclic loading case has the following variation with time:

$$V(t) = 300\,sin^2(\pi t/T), H(t/T) = 0$$

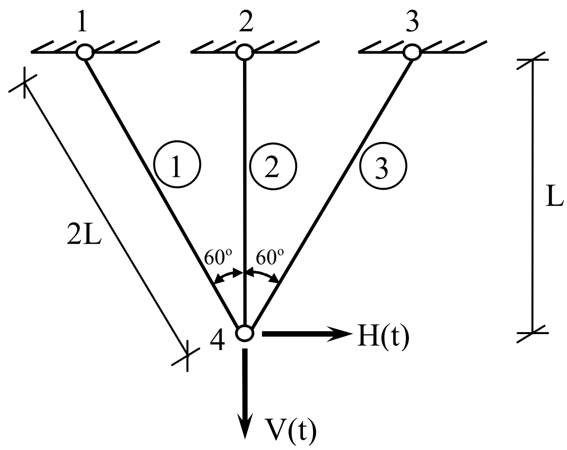

Figure 1: Three bar truss example

The analysis shows that bar *2* yields in tension and bars *1*, *3* remain elastic. As it may be observed, the residual stress remains constant inside the cycle (Fig. 2), therefore this load case leads to elastic adaptation. The cyclic steady state residual stress distribution for the element *2* inside a cycle may be seen in Fig. 2.

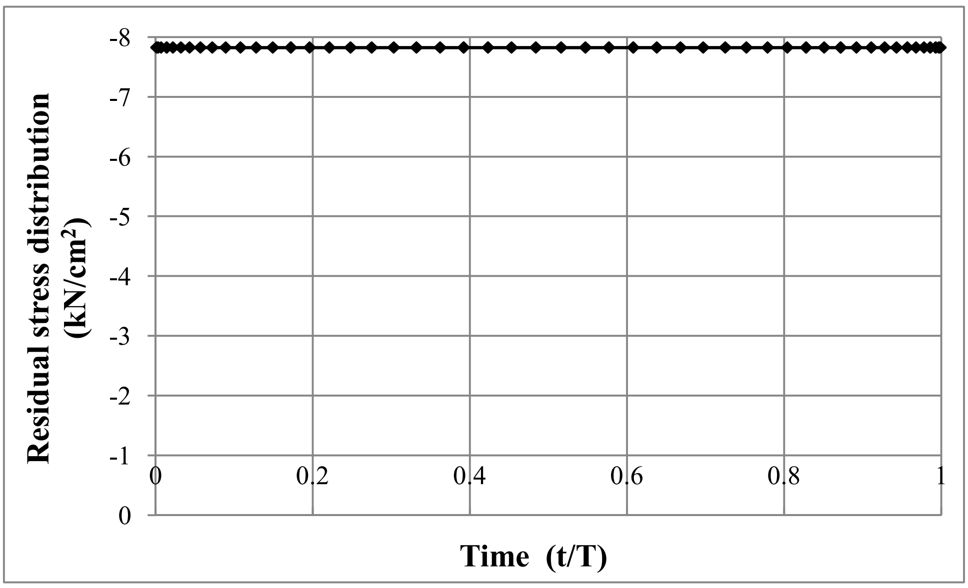

Figure 2: Cyclic state residual stress distribution inside a cycle for load case a (element 2)

b) The second cyclic loading case has the following variation with the time:

$$V(t) = 300\sin(2\pi t / T), H(t/T) = 0$$

The analysis shows that during the first half of the cycle bar *2* yields in tension and during the second half, bar *2* yields in compression. We also see that the plastic strain rates for the bar *2* are equal and of opposite sign in the first and second half of the cycle. Therefore this load case leads the structure to alternating plasticity. The cyclic steady state residual stress distribution for the element *2* inside a cycle may be seen in Fig. 3.

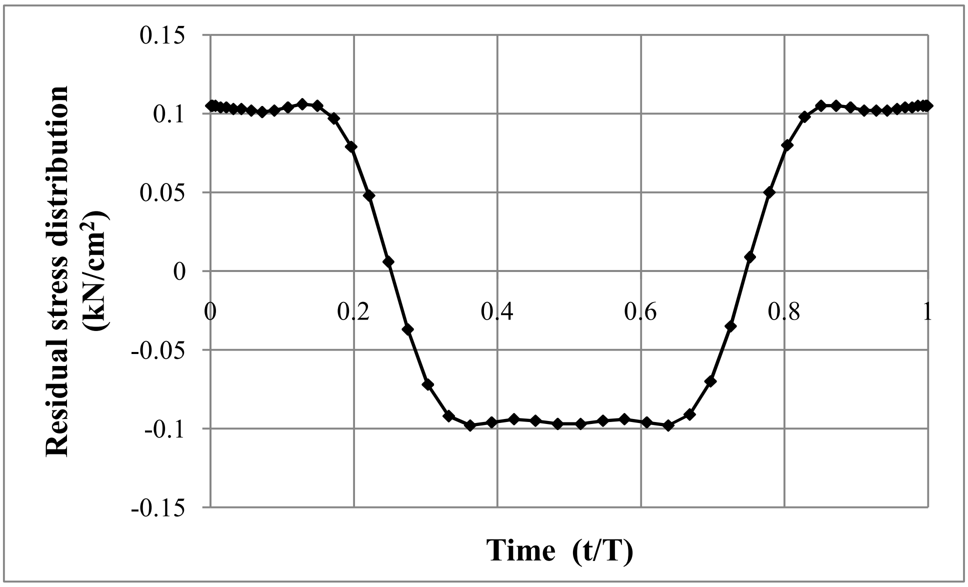

Figure 3: Cyclic state residual stress distribution inside a cycle for load case b (element 2)

c) The third cyclic loading case includes a variation with time of both the vertical and the horizontal load:

$$V(t) = 350\,sin^2(\pi t / T),\ H(t) = 220\,sin(2\pi t / T)$$

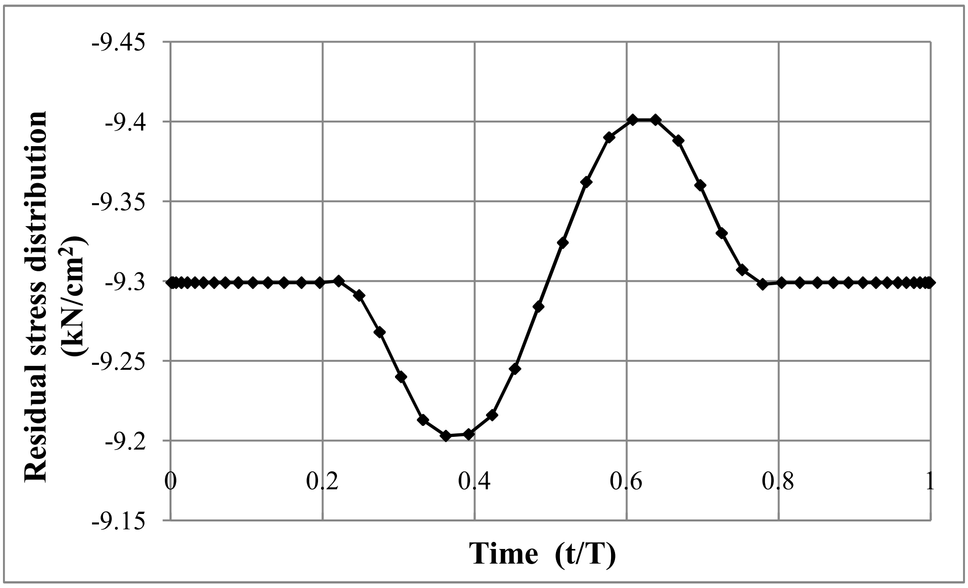

Figure 4: Cyclic state residual stress distribution inside a cycle for load case c (element 2)

The results obtained by the analysis show that during the first half of the cycle bar *2* yields in tension and during the second half bar *3* yields also in tension. Also the value

$a = \left\| \int_0^T \Delta\boldsymbol{\sigma}^{(\mu)}(t)dt \right\|$ referred to in the numerical procedure which is an indirect measure of the total change in plastic strains over the cycle is non zero; therefore this load case leads the structure to incremental collapse. The cyclic steady state residual stress distribution inside a cycle for the element *2* may be seen in Fig. 4.

5.2 Square plate with a hole

The second example of application is a plane stress concentration problem of a square plate with dimensions $20 \times 20cm$ and having a circular hole in its middle of a diameter of $2cm$. The loading is applied in equal pairs along the two vertical edges of the plate. Due to the symmetry of the structure and the loading we only analyze one quarter of the structure with $a = 10cm$ and $b = 1cm$. Ninety-eight 8-noded isoparametric elements with 3×3 Gauss integration points were used for the finite element discretization (Fig. 5).

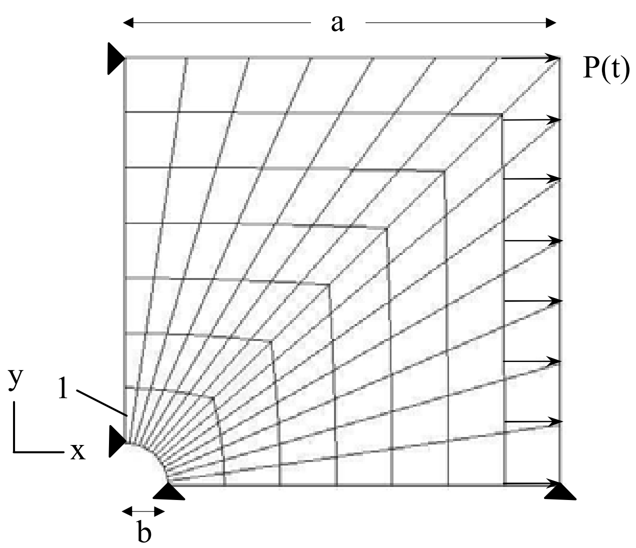

Figure 5: Finite element discretization of a quarter of a plate

The following material data was used: Young's modulus $E = .21 \times 10^5 kN / cm^2$ and yield stress $\sigma_y = 24kN / cm^2$. Two cases of loading have been considered that leads the plate to either elastic shakedown or alternating plasticity. The cyclic steady state residual stress distribution inside a cycle for the Gauss point *1* may be seen in Fig. 6, 7. This point is the nearest integration point to the corner where the longitudinal elastic stress is maximum.

a) The first cyclic loading case has the following variation with time where the maximum value of the cyclic loading is $P_0 = 20kN$:

$$P(t) = P_0 * sin^2\left(\pi \frac{t}{T}\right)$$

The cyclic steady-state residual stress distribution inside a cycle for Gauss point *1* may be seen in Fig. 6. As it may be observed, the residual stress remains constant inside the cycle. Therefore this load case leads to elastic adaptation.

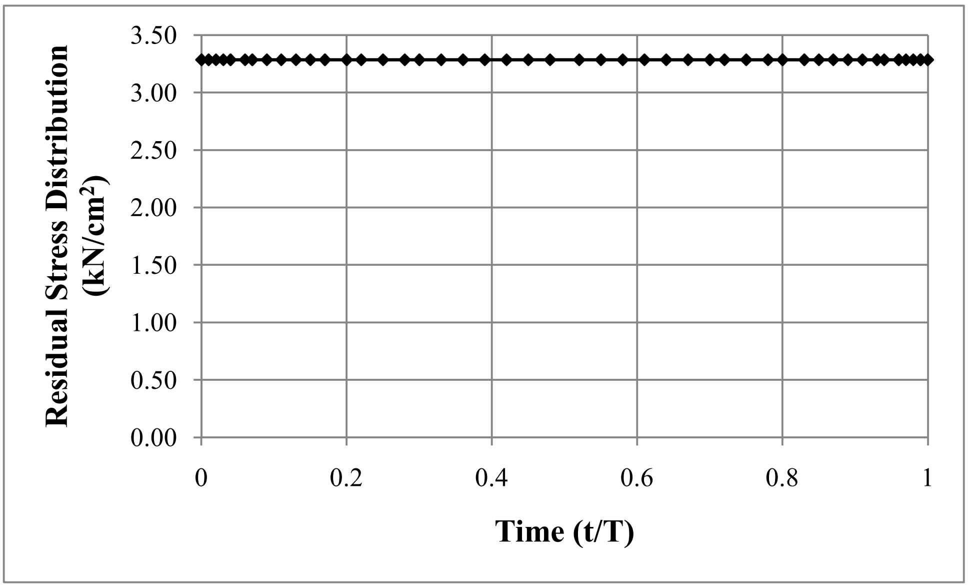

Figure 6: Cyclic state residual stress distribution inside a cycle for load case b (Gauss point 1)

b) The second cyclic loading case has the above variation with time while the maximum value of the cyclic loading being $P_0 = 20kN$:

$$P(t) = P_0 * sin\left(2\pi \frac{t}{T}\right)$$

The cyclic steady-state residual stress distribution inside a cycle for Gauss point *1* may be seen in Fig. 7. We also see that the plastic strain rates for the Gauss point *1* are equal and of opposite sign in the first and second half of the cycle. Therefore this load case leads the structure to alternating plasticity.

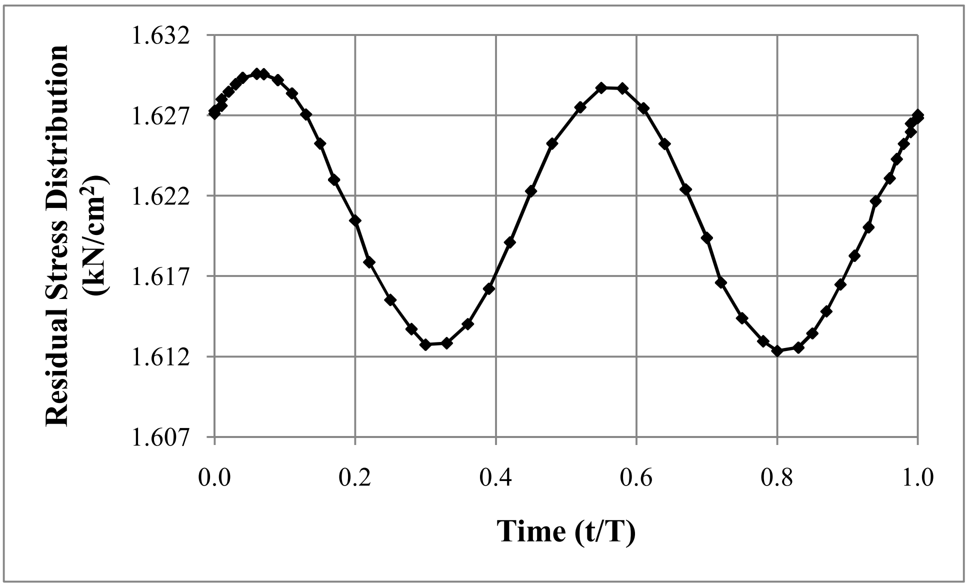

Figure 7: Cyclic state residual stress distribution inside a cycle for load case b (Gauss point 1)

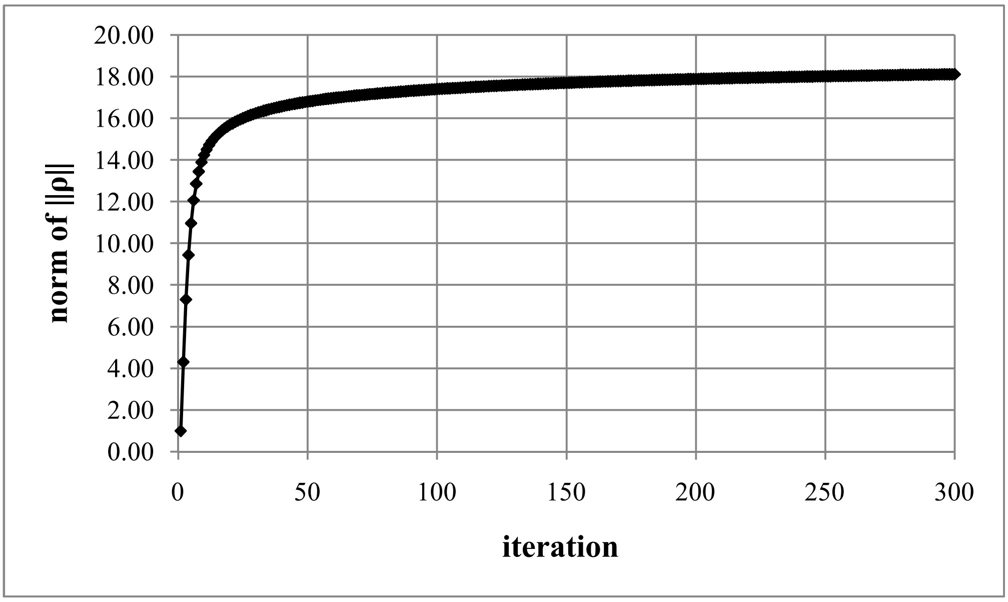

Figure 8: Norm variation with iterations (second example – incremental collapse case)

In Fig.8 one can see the convergence characteristics of the proposed method. It may be realized that the approach is very stable and with uniform convergence.

The observed behaviour of elastic shakedown, alternating plasticity or incremental collapse for both the one and two dimensional examples was found to coincide with the one obtained by a time-stepping finite element program, (ABAQUS [10]). Within [10] an explicit time integration scheme was considered and in order to get higher accuracy this time stepping program had to go through many time increments to get the steady-state solution and to predict the cyclic behavior of the structure, especially for the second example.

6 CONCLUSIONS

- In the present work a direct method is proposed that may be used for the cyclic steady state elastoplastic analysis of structures under cyclic loading.
- It is based on the decomposition of the residual stress distribution into Fourier series whose coefficients are calculated by iterations.
- The method allows approaching directly the long-term effects on the structure without following laborious time-stepping calculations.
- A very few number of terms of the Fourier series generally proved sufficient.
- A limited number of time points inside the cycle are needed, mainly to properly describe the time variation of the cyclic load.
- For all the examples that were presented above the cyclic steady-state was reached in a few iterations.
- The stiffness matrix needs to be formulated and decomposed only once.
- The procedure is stable and has uniform convergence.

REFERENCES

[1] Frederic C.O. and Armstrong P.J. Convergent internal stresses and steady cyclic states of stress. *J. Strain. Anal*. (1966) **1**: 154-169.

[2] Andersen E.D., Roos C., Terlaky T. On implementing a primal-dual interior-point method for conic quadratic optimization. *Math. Program. Ser. B* (2003) **95**: 249–277.

[3] Weichert D. and Hachemi A. Progress in the application of lower bound direct methods in structural design. *Int. J. Appl. Mech*. (2010) **2**: 145-160.

[4] Tran T.N., Liu G.R., Nguyen-Xuan H., Nguyen-Toi T. An edge-based smoothed finite element method for primal–dual shakedown analysis of structures. *Int. J. Numer. Meth. Engng.* (2010) **82**:917–938.

[5] Casciaro R. and Garcea G. An iterative method for shakedown analysis. *Comput. Methods Appl. Mech. Engrg.* (2002) **191**: 5761–5792.

[6] Ponter A.R.S. and Chen H. A minimum theorem for cyclic load in excess of shakedown, with application to the evaluation of a ratchet limit. *Eur. J. Mech. A/Solids* (2001) **20**: 539-553.

[7] Chen H. and Ponter A.R.S. A method for the evaluation of a ratchet limit and the amplitude of plastic strain for bodies subjected to cyclic loading. *Eur. J. Mech. A/Solids* (2001) **20**: 555–571.

[8] Ponter A.R.S. The linear matching method for limit loads, shakedown limits and ratchet limits. In Weichert D. and Ponter A. (eds.) *Limit states of materials and structures*. Springer (2009).

[9] Spiliopoulos K.V. A simplified method to predict the steady cyclic stress state of creeping structures. *ASME J. Appl. Mech*. (2002) **69**:148-153.

[10] ABAQUS 6.10. *User's Manual*. Dassault Systèmes Simulia Corp., Providence, RI, USA (2010)